1

Adaptive Finite Element Methods for Flow Problems

Roland Becker, Malte Braack and Rolf Rannacher
Institut für Angewandte Mathematik, Universität Heidelberg
`http://gaia.iwr.uni-heidelberg.de`

Abstract

We present a general approach to error control and mesh adaptation for computing viscous flows by the Galerkin finite element method. A posteriori error estimates are derived for quantities of physical interest by duality arguments. In these estimates local cell residuals are multiplied by influence factors which are obtained from the numerical solution of a global dual problem. This provides the basis of a feed-back algorithm by which economical meshes can be constructed which are tailored to the particular needs of the computation. The performance of this method is illustrated by several flow examples.

1.1 Introduction

Approximating partial differential equations by discretization as in the finite element method may be considered as a *model reduction* where a conceptually *infinite* dimensional model is approximated by a *finite* dimensional one. As the result of the computation, we obtain an approximation to the desired output quantity of the simulation and besides that certain accuracy indicators like cell-residuals. Controlling the error in such an approximation of a continuous model requires to determine the influence factors for the *local* error indicators on the target quantity. Such a sensitivity analysis with respect to local perturbations of the model is common in optimal control theory and introduces the concept of a *dual* (or *adjoint*) problem.
For illustration, let $Lu = f$ be a (linear) differential problem posed in variational form and $L_h u_h = f_h$ its approximation by a Galerkin finite element method on a meshes $\mathcal{T}_h = \{K\}$ with cells K. Then, the error

$e := u - u_h$ satisfies $Le = \rho$ in the variational sense with the "residual" $\rho := f - Lu_h$ as right-hand side. Now, let $J(u)$ be a quantity of physical interest derived from the solution u by applying a functional $J(\cdot)$. The goal is to control the error of the discretization with respect to this functional output in terms of certain computable cell residuals $\rho_K(u_h)$. An example is control of the total error $e_K = u - u_{h|K}$ in some cell K. By superposition, e_K splits into two components, the locally produced *truncation error* and the globally transported *pollution error*, i.e., $e_K^{\rm tot} = e_K^{\rm loc} + e_K^{\rm trans}$. This asks for control of

- error propagation in space (global pollution effect),
- interaction of physical error sources (local sensitivity analysis).

Clearly, the effect of the cell residual ρ_K on the local error $e_{K'}$, at another cell K', is governed by a Green function of the continuous problem which is determined globally by the adjoint operator. Capturing this dependence by *numerical* evaluation is the general philosophy underlying our approach to error control. In this it differs essentially from the traditional method which is based on local residual-type information alone (see [22] and [1] for surveys). In practice it is mostly impossible to determine the complex error interaction by analytical means, it rather has to be detected by computation. This eventually results in a feed-back process in which error estimation and mesh adaptation goes hand-in-hand leading to economical discretization for computing the quantities of interest with high accuracy.

1.2 A general paradigm for a posteriori error estimation

We outline our concept of error estimation in an abstract setting following the general paradigm introduced in Johnson [18] and in Eriksson/Estep/Hansbo/Johnson [12]. For a detailed discussion of the practical aspects of this approach, we refer to [8] and [9]; a survey with applications to various problems in mechanics and physics has been given in [20]. Here, we concentrate on the aspects particularly relevant for flow computations.

Let $\hat{V}$ be a Hilbert space with inner product $(\cdot,\cdot)$ and corresponding norm $\|\cdot\|$, $V \subset \hat{V}$ a subspace with dual V^* and $A(\cdot;\cdot)$ a continuous semi-linear form on $\hat{V}\times\hat{V}$. Further, let $\hat{u} \in \hat{V}$ be a particular element representing prescribed boundary data. For a given $F \in V^*$, we seek a

solution $u \in V+\hat{u}$ to the abstract variational problem

$$A(u;\varphi) = F(\varphi) \qquad \forall\, \varphi \in V. \tag{2.1}$$

This problem is approximated by a Galerkin method using a sequence of finite dimensional subspaces $V_h \subset \hat{V}_h \subset \hat{V}$ indexed by a discretization parameter h. The discrete problems seek $u_h \in V_h+\hat{u}_h$, satisfying

$$A(u_h;\varphi_h) = F(\varphi_h) \qquad \forall\, \varphi_h \in V_h. \tag{2.2}$$

The key feature of this approximation is the "Galerkin orthogonality" which in this nonlinear case is expressed as

$$A(u;\varphi_h) - A(u_h;\varphi_h) = 0, \quad \varphi_h \in V_h. \tag{2.3}$$

By elementary calculus, there holds

$$A(u;\varphi_h) - A(u_h;\varphi_h) = \int_0^1 A'(su + (1-s)u_h; e, \varphi_h)\, ds,$$

with $A'(v;\cdot,\cdot)$ denoting the tangent form of $A(\cdot;\cdot)$ at some $v \in \hat{V}$. This leads us to introduce the bilinear form

$$L(u, u_h; \varphi, \psi) := \int_0^1 A'(su + (1-s)u_h; \varphi, \psi)\, ds\,,$$

which depends on the solutions u as well as u_h. Then, for the error $e = u-u_h$, there holds

$$\begin{aligned} L(u, u_h; e, \varphi_h) &= \int_0^1 A'(su + (1-s)u_h; e, \varphi_h)\, ds \\ &= A(u;\varphi_h) - A(u_h;\varphi_h) = 0\,, \quad \varphi_h \in V_h\,. \end{aligned}$$

Suppose that the quantity $J(u)$ has to be computed, where $J(\cdot)$ is a linear functional on V. For representing the error $J(e)$, we use the solution $z \in V$ of the following so-called "dual problem":

$$L(u, u_h; \varphi, z) = J(\varphi) \qquad \forall\, \varphi \in V, \tag{2.4}$$

assuming that this problem is solvable. Taking $\varphi = e$ in (2.4) and using the Galerkin orthogonality (2.3), we obtain the error representation

$$J(e) = L(u, u_h; e, z - \varphi_h) = F(z-\varphi_h) - A(u_h; z-\varphi_h), \tag{2.5}$$

with an arbitrary $\varphi_h \in V_h$. This simple argument assumes that $e \in V$ which requires exact representation of boundary data, i.e., $\hat{u} = \hat{u}_h$. In practice this condition may not be satisfied which requires modifications in the argument using the particular structure of the problem (see the

example in the next section). Since the bilinear form $L(u,u_h;\cdot,\cdot)$ contains the unknown solution u in its coefficient, the evaluation of (2.5) requires approximation. The simplest way is to replace u by u_h, yielding a perturbed dual bilinear form

$$L(u_h,u_h;\varphi,\psi) = A'(u_h;\varphi,\psi).$$

Controlling the effect of this perturbation on the accuracy of the resulting error estimator may be a delicate task and depends strongly on the particular problem considered. Our own experience with several different types of problems (including the Navier-Stokes equations) indicates that this problem is less critical as long as the continuous solution is stable. The crucial problem is the numerical solution of the linearized dual problem. To this end, we may select certain subspaces $\tilde{V}_h \subset V$ and compute an approximation $\tilde{z}_h \in \tilde{V}_h$ by solving

$$L(u_h,u_h;\varphi_h,\tilde{z}_h) = J(\varphi_h) \qquad \forall\,\varphi_h \in \tilde{V}_h. \tag{2.6}$$

In practice, we may require $V_h \subset \tilde{V}_h$ or even $V_h = \tilde{V}_h$. The effect of all these approximations is described in the following theorem.

Theorem 1.2.1 *Let $z \in V$ be the solution of the linearized dual problem*

$$A'(u_h;\varphi,z) = J(\varphi) \quad \forall\varphi \in V. \tag{2.7}$$

Then, there holds the a posteriori error representation

$$J(e) \;=\; F(z-\varphi_h) - A(u_h,z-\varphi_h) + R(u,u_h;e,e,z), \tag{2.8}$$

with an arbitrary $\varphi_h \in V_h$, and a remainder term

$$R(u,u_h;e,e,z) := \int_0^1 A''(u_h+se;e,e,z)\,(1-s)\,ds.$$

Proof. Setting $\varphi = e$ (assuming $e \in V$) in the dual problem (2.7), we obtain

$$J(e) = A'(u_h;e,z).$$

Further, noting that

$$A(u;z) = A(u_h;z) + A'(u_h;e,z) + \int_0^1 A''(u_h+se;e,e,z)\,(1-s)\,ds,$$

and $A(u;z) = F(z)$, we conclude

$$J(e) = F(z) - A(u_h;z) + R(u,u_h;e,e,z),$$

with the remainder term

$$R(u,u_h;e,e,z) := \int_0^1 A''(u_h+se;e,e,z)\,(1-s)\,ds.$$

Then, using the Galerkin orthogonality (2.3), we obtain

$$J(e) = F(z-\psi_h) - A(u_h;z-\psi_h) + R(u,u_h;e,e,z),$$

for an arbitrary $\varphi_h \in V_h$. □

Clearly, the remainder term R in (2.8) vanishes if $A(\cdot;\cdot)$ is affine-linear. We note, that Theorem 1.2.1 allows a natural generalization to cover also the case of a nonlinear, differentiable error functional $J(\cdot)$.

1.2.1 The solution approach

The approximation of problem (2.1) by a Galerkin method has been described in a functional analytic setting. For actually solving it on a computer, we have to convert the *discrete* problem (2.2) into an algebraic equation. To this end, we choose a basis $\{\varphi^\nu,\ \nu=1,...,N=\dim V_h\}$ of the subspace $V_h \subset V$ (for instance the standard "nodal function basis" in a finite element scheme) and seek for a solution in the form

$$u_h = \sum\nolimits_{\nu=1}^{N} x_\nu \varphi^\nu + \hat{u}_h\,.$$

Inserting this ansatz into equation (2.2) results in a nonlinear algebraic system

$$A(u_h;\varphi^\nu) = F(\varphi^\nu), \quad \nu = 1,...,N. \tag{2.9}$$

for the unknown coefficient vector $x = \{x_\nu\}_{\nu=1}^N$. This may be solved for instance by a Newton iteration. In the context of adaptive discretization, this solution process is usually coupled with successive mesh refinement. The resulting *nested* algorithm reads as follows.

Let a desired error tolerance TOL or a maximum mesh complexity $N_{\max}$ be given. Starting from a coarse initial mesh $\mathcal{T}_0$, a hierarchy of successively refined meshes $\mathcal{T}_i,\ i \geq 1$, and corresponding finite element spaces $V_i \subset \hat{V}_i$ is generated as follows:
(0) *Initialization* $i = 0$: Compute an initial approximation $u_0 \in \hat{V}_0$.
(i) *Defect correction iteration:* For $i \geq 1$, start with $u_i^{(0)} := u_{i-1} \in \hat{V}_i$.
(ii) *Iteration step:* For $j \geq 0$ evaluate the defect

$$(d_i^{(j)},\varphi) := F(\varphi) - A(u_i^{(j)};\varphi), \quad \varphi \in V_i. \tag{2.10}$$

Choose a suitable approximation $\tilde{A}'(u_i^{(j)};\cdot,\cdot)$ to $A'(u_i^{(j)};\cdot,\cdot)$ (with good

stability and solubility properties) and compute a correction $v_i^{(j)} \in V_i$ from the linear equation

$$\tilde{A}'(u_i^{(j)}; v_i^{(j)}, \varphi) = (d_i^{(j)}, \varphi) \quad \forall \varphi \in V_i. \tag{2.11}$$

For this, Krylov-space or multigrid methods are employed using the hierarchy of meshes $\{\mathcal{T}_i, ..., \mathcal{T}_0\}$. Then, update $u_i^{(j+1)} = u_i^{(j)} + \lambda_i v_i^{(j)}$, with some relaxation parameter $\lambda_i \in (0, 1]$, set $j := j+1$ and go back to (2). This process is repeated until a limit $\tilde{u}_i \in \hat{V}_i$, is reached with a certain prescribed accuracy.

(iii) *Error estimation:* Accept $u_i := \tilde{u}_i$ as the solution on mesh $\mathcal{T}_i$ and solve the discrete linearized dual problem

$$z_i \in V_i : \quad A'(u_i; \varphi, z_i) = J(\varphi) \quad \forall \varphi \in V_i, \tag{2.12}$$

and evaluate the a posteriori error estimate

$$|J(e_i)| \approx \eta(u_i). \tag{2.13}$$

For controlling the reliability of this bound, i.e. the accuracy in the determination of the dual solution z, one may check whether the change $\|z_i - z_{i-1}\|$ is sufficiently small; if this is not the case, additional global mesh refinement is advisable. If $\eta(u_i) \leq TOL$ or $N_i \geq N_{\max}$, then stop. Otherwise, cell-wise mesh adaptation yields the new mesh $\mathcal{T}_{i+1}$. Then, set $i := i+1$ and go back to (i).

We note that the evaluation of the a posteriori error estimate (2.13) involves only the solution of *linearized* problems. Hence, the whole error estimation may amount only to a relatively small fraction of the total cost for the solution process. This has to be compared to the usually much higher cost when working on non-optimized meshes.

In using the a posteriori error estimate (2.13), it is assumed that the exact discrete solution $u_i \in V_i$ on mesh $\mathcal{T}_i$ is available. This asks for estimation of the unavoidable iteration error $\tilde{u}_i - u_i$ and its effect on the accuracy of the estimator for the discretization error. This can be achieved in the case of a Galerkin finite-element multigrid iteration by exploiting the projection properties of the combined scheme (see [3]).

1.3 Practical realization of error control

1.3.1 Evaluation of a posteriori error estimates

Next, we want to discuss how the abstract a posteriori error representation (2.8) is evaluated and used in mesh refinement in practice. To this

end, we consider the usual scalar Laplace equation

$$-\Delta u = f \quad \text{in } \Omega, \quad u_{|\partial\Omega} = \hat{u}, \tag{3.14}$$

on a polygonal domain $\Omega \subset \mathbb{R}^2$ with boundary $\partial\Omega$, and some prescribed right-hand side $f \in L^2(\Omega)$ and sufficiently smooth boundary value $\hat{u}$.

Before proceeding, let us fix some notation. We will denote by $(\cdot,\cdot)_D$ the L^2 scalar product on some domain D and by $\|\cdot\|_D$ the corresponding norm; in the case $D = \Omega$, the subscript D is usually omitted. Further, we use the standard notation $L^2(D)$ for the Lebesgue space as well as $H^1(D)$ and $H_0^1(D)$ for the first-order Sobolev spaces over D.

For the following, we set $\hat{V} := H^1(\Omega)$ and $V := H_0^1(\Omega)$. Then, the variational formulation of (3.14) seeks $u \in V + \hat{u}$ satisfying

$$A(u;\varphi) := (\nabla u, \nabla\varphi) = (f,\varphi) \quad \forall\varphi \in V. \tag{3.15}$$

We consider the approximation of (3.15) by a standard Galerkin finite element method. To fix ideas, let us consider only piecewise *bilinear* shape functions defined on quasi-regular rectangular meshes $\mathcal{T}_h = \{K\}$ consisting of non-degenerate cells K (rectangles) with edges denoted by Γ, as described in the standard finite element literature; see, e.g., Johnson [17]. The local mesh width is denoted by $h_K = \operatorname{diam}(K)$ and $h := \max_{K\in\mathcal{T}_h} h_K$. In order to facilitate local mesh refinement and coarsening, we allow the cells in the refinement zone to have nodes which lie on faces of neighboring cells (Fig. 1.1). The degrees of freedom corresponding to such "hanging nodes" are eliminated from the system by interpolation inforcing global conformity (i.e., continuity across interelement boundaries) for the finite element functions.

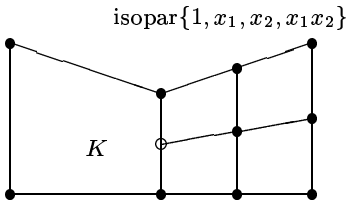

Fig. 1.1. Quadrilateral mesh patch with a "hanging node"

In this setting, the error representation (2.8) can be developed into a more concrete form. Since the form $A(\cdot;\cdot)$ is linear in this case, the nonlinear remainder term vanishes. The dual problem corresponding to

a (linear) error functional $J(\cdot)$ seeks a $z \in V$ such that

$$(\nabla\varphi, \nabla z) = J(\varphi) \quad \forall\varphi \in V. \tag{3.16}$$

We do not want to assume that $\hat{u}_h = \hat{u}$, so that $e = u - u_h \notin V$. Hence, we cannot directly take $\varphi = e$ as test function in (3.16). We deal with this complication by rewriting (3.16) in the form

$$(\nabla\varphi, \nabla z) - (\varphi, \partial_n z)_{\partial\Omega} = J(\varphi), \quad \varphi \in \hat{V}. \tag{3.17}$$

Taking here $\varphi = e$ yields

$$J(e) = (\nabla e, \nabla z) - (\hat{u} - \hat{u}_h, \partial_n z)_{\partial\Omega}.$$

On the first term on the right, we can now use the Galerkin orthogonality and cell-wise intergartion by parts, to obtain

$$\begin{aligned}(\nabla e, \nabla z) &= (\nabla e, \nabla(z - \varphi_h)) \\ &= \sum\nolimits_{K\in\mathcal{T}_h} \big\{(f + \Delta u_h, z - \varphi_h)_K - (\partial_n u_h, z - \varphi_h)_{\partial K}\big\}, \\ &= \sum\nolimits_{K\in\mathcal{T}_h} \big\{(R(u_h), z - \varphi_h)_K + (r(u_h), z - \varphi_h)_{\partial K}\big\},\end{aligned}$$

with an arbitrary $\varphi_h \in V_h$. Here, the "equation residual" $R(u_h)$ and the "jump residual" $r(u_h)$ are cellwise defined by

$$R(u_h)_{|K} := f + \Delta u_h, \quad r(u_h)_{|\Gamma} := \begin{cases} -\frac{1}{2}[\partial_n u_h], & \text{if } \Gamma \not\subset \partial\Omega, \\ -\partial_n u_h, & \text{if } \Gamma \subset \partial\Omega. \end{cases}$$

Here, $[\partial_n u_h]$ denotes the jump of $\partial_n u_h$ across the edge Γ. This error representation may be directly evaluated if a good approximation $\tilde{z} \sim z$ is available. This can be achieved by solving the dual problem either on a finer mesh or by patchwise higher-order interpolation of its approximation on the same mesh. For a systematic study of these alternatives, we refer to [9]. In order to derive cell error indicators which can be used in the mesh refinement process, we have to convert the error representation into an estimate. Using Hölder's inequality, we obtain the a posteriori error estimate

$$|J(e)| \le \sum\nolimits_{K\in\mathcal{T}_h} \big\{\rho_K\omega_K + \rho_{\partial K}\omega_{\partial K}\big\} + |(\hat{u} - \hat{u}_h, \partial_n z)_{\partial\Omega}|, \tag{3.18}$$

with the cell residuals and corresponding weights defined by

$$\begin{aligned}\rho_K &:= \|R(u_h)\|_K, \quad \rho_{\partial K} := h_K^{-1/2}\|r(u_h)\|_{\partial K}, \\ \omega_K &:= \|z - I_h z\|_K, \quad \omega_{\partial K} := h_K^{1/2}\|z - I_h z\|_{\partial K},\end{aligned}$$

where $I_h z \in V_h$ is a suitable nodal interpolation of the dual solution z.

Normally, the dual problem is solved by the same method as used for the primal problem resulting in an approximation $z_h \in V_h$. In this case, we replace the difference $z - I_h z$ in the error estimate (3.18) in terms of the local interpolation estimate

$$\max\left\{\|z - I_h z\|_K,\ h_K^{1/2}\|z - I_h z\|_{\partial K}\right\} \le c_I h_K^2 \|\nabla^2 z\|_K, \tag{3.19}$$

with an interpolation constant $c_I \sim 1$. In turn, the second derivative of the dual solution is replaced by a suitable second-order difference quotient of its computed approximation,

$$\|\nabla^2 z\|_K \approx \|\nabla_h^2 z_h\|_K. \tag{3.20}$$

This results in the approximate a posteriori error estimate

$$|J(e)| \approx c_I \sum\nolimits_{K\in\mathcal{T}_h} h_K^2 \tilde{\rho}_K \tilde{\omega}_K + |(\hat{u} - \hat{u}_h, \partial_n z)_{\partial\Omega}|, \tag{3.21}$$

where $\tilde{\rho}_K := \rho_K + \rho_{\partial K}$ and $\tilde{\omega}_K := \|\nabla_h^2 z_h\|_K$. In concrete applications the cell-wise parts of the boundary term in the estimator are smaller than the interior indicators. Nevertheless, they may lead to mesh refinement along the inflow boundary as can be seen in the flow examples presented below.

We recall the interpretation of this a posteriori error estimate. On each cell, we have an "equation residual" $R(u_h)$ and a "flux residual" $r(u_h)$, the latter one expressing smoothness of the discrete solution. Both residuals can easily be evaluated. They are multiplied by the weights $\tilde{\omega}_K$ which provide quantitative information about the impact of these cell-residuals on the error $J(e)$ in the target quantity (*sensitivity factors*).

1.3.2 Mesh adaptation strategies

Now, we want to discuss some popular strategies for mesh adaptation based on an a posteriori error estimate of the form

$$|J(e)| \le \eta := \sum\nolimits_{K\in\mathcal{T}_h} \eta_K, \tag{3.22}$$

with certain cell-error indicators $\eta_K = \eta_K(u_h)$ obtained on the current mesh $\mathcal{T}_h$. Suppose that a tolerance TOL for the error $J(e)$ or a maximum number $N_{\max}$ of mesh cells have been prescribed. Starting from an approximate solution $u_h \in V_h + \hat{u}_h$ obtained on the current mesh $\mathcal{T}_h$ the mesh adaptation may be organized by one of the following strategies.

- *Error balancing strategy:* Cycle through the mesh and equilibrate the local error indicators according to $\eta_K \approx \mathrm{TOL}/N$ with $N := \#\{K \in \mathcal{T}_h\}$. This leads eventually to $\eta \approx TOL$, but requires iteration with respect to N.
- *Fixed fraction strategy:* Order cells according to the size of η_K and refine a certain percentage (say 30%) of cells with largest η_K (or those which make up 30% of the estimator value η) and coarsen those cells with smallest η_K. By this strategy, we may achieve a prescribed rate of increase of N.
- *Mesh optimization strategy:* Use the (assumed) representation

$$\eta := \sum\nolimits_{K\in\mathcal{T}_h} \eta_K \approx \int_\Omega h(x)^2 \Phi(x)\, dx \tag{3.23}$$

for directly generating a formula for an optimal mesh-size distribution:

$$h_{opt}(x) = \Big(\frac{W}{N_{\max}}\Big)^{1/2} \Phi(x)^{-1/4}, \quad W := \int_\Omega \Phi(x)^{1/2}\, dx. \tag{3.24}$$

Here, we think of a smoothly distributed mesh-size function $h(x)$ such that $h_{|K} \approx h_K$. The existence of such a representation with an h-independent error density function $\Phi(x) = \Phi(u(x), z(x))$ can be rigorously justified only under very restrictive conditions but is generally supported by computational experience (for details see [9]).

1.4 Application to incompressible fluid flow

As the first application, we consider a viscous incompressible Newtonian fluid flow modeled by the (stationary) Navier-Stokes equations

$$-\nu\Delta v + v\cdot\nabla v + \nabla p = f, \qquad \nabla\cdot v = 0\,, \tag{4.25}$$

for the velocity v and the pressure p in a bounded domain $\Omega \subset \mathbb{R}^2$. Here, $\nu >$ is the normalized viscosity (density $\rho \equiv 1$), and the volume force is assumed as $f \equiv 0$. At the boundary $\partial\Omega$, the usual non-slip condition is imposed along rigid parts together with suitable inflow and free-stream outflow conditions,

$$v|_{\Gamma_{\rm rigid}} = 0, \quad v|_{\Gamma_{\rm in}} = \hat{v}, \quad \nu\partial_n v - pn|_{\Gamma_{\rm out}} = 0.$$

In the following, vector functions are also denoted by normal type and no distinction is made in the notation of the corresponding inner products and norms.

As an example, we consider the flow around the cross section of a

cylinder with surface S in a channel with a narrowed outlet (see Fig. 1.2). Here, a quantity of physical interest is for example the "drag coefficient" defined by

$$J_{\text{drag}}(v,p) := \frac{2}{\hat{V}^2 D} \int_S n \cdot \sigma(v,p) \psi \, ds, \tag{4.26}$$

where $\psi := (0,1)^T$, $\sigma(v,p) = \frac{1}{2}\nu(\nabla v + \nabla v^T) + pI$ *is* the stress acting on the cylinder, D is its diameter, and $\hat{V} := \max|\hat{v}|$ is the reference velocity. In this example, the Reynolds number is $\text{Re} = \hat{V}^2 D/\nu = 50$, such that the flow is stationary.

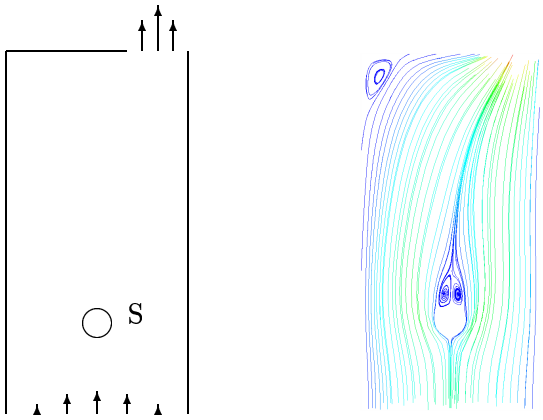

Fig. 1.2. Configuration and streamline plot of the "flow around a cylinder"

The variational formulation of (4.25) uses the function spaces

$$\hat{V} := L \times \hat{H}, \quad V := L \times H \subset \hat{V},$$

where $L := L^2(\Omega)$, $\hat{H} := H^1(\Omega)^2$, and $H := \{v \in \hat{H},\ v_{|\Gamma_{\text{in}} \cup \Gamma_{\text{rigid}}} = 0\}$. In the special case $\Gamma_{\text{out}} = \emptyset$, we set $L := \{q \in L^2(\Omega),\ \int_\Omega q \, dx = 0\}$. For $u = \{p, v\}$, $\varphi = \{q, w\} \in \hat{V} \times \hat{V}$, we define the bilinear form

$$A(u;\varphi) := (\nabla u, \nabla w) + (v \cdot \nabla v, w) - (p, \nabla \cdot w) + (q, \nabla \cdot v)$$

and seek $u = \{p, v\} \in V + \{0, \hat{v}\}$, such that

$$A(u;\varphi) = (f, w) \quad \forall \varphi = \{q, w\} \in V. \tag{4.27}$$

For discretizing this problem, we use a finite element method based on the quadrilateral Q_1/Q_1-Stokes element with globally continuous (piecewise isoparametric) bilinear shape functions for both unknowns, pressure and velocity. As described before, we allow "hanging" nodes while the

corresponding unknowns are eliminated by linear interpolation. The corresponding finite element subspaces are denoted by

$$L_h \subset L, \quad \hat{H}_h \subset \hat{H}, \quad H_h \subset H, \quad \hat{V}_h := L_h \times \hat{H}_h, \quad V_h := L_h \times H_h,$$

and $\hat{v}_h \in \hat{H}_h$ is a suitable interpolation of the boundary function $\hat{v}$. This construction is oriented by the situation of a polygonal domain Ω for which the boundary $\partial\Omega$ is exactly matched by the mesh domain $\Omega_h := \cup\{K \in \mathcal{T}_h\}$. In the case of a general curved boundary (as in the above flow example) some standard modifications are necessary which are omitted here for the sake of brevity.

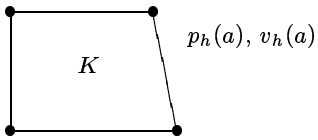

Fig. 1.3. The Q_1/Q_1-Stokes element

In order to obtain a stable discretization of (4.27) in these spaces with "equal-order interpolation" of pressure and velocity, we use the least-squares technique proposed in [16]. Following [15] a similar approach is employed for stabilizing the convective term. The Navier-Stokes system can be written in vector form for the unknown $u = \{p, v\}$ like

$$A(u) := \begin{bmatrix} -\nu\Delta v + v\cdot\nabla v + \nabla p \\ \nabla\cdot v \end{bmatrix} = \begin{bmatrix} f \\ 0 \end{bmatrix} =: F.$$

The operator $A(\cdot)$ has a differential at u which acts on elements $\varphi = \{q, w\} \in \hat{V}$ like

$$A'(u)\varphi := \begin{bmatrix} -\nu\Delta w + v\cdot\nabla w + w\cdot\nabla v + \nabla q \\ \nabla\cdot w \end{bmatrix}.$$

For stabilizing the formulation (4.27) and also for preconditioning in the linear defect equations (2.11), we use the following simplification of $A'(u)$ (suitable for low-order finite elements) which avoids the presence of the "reaction term" $w\cdot\nabla v = (\nabla v)^T w$:

$$\tilde{A}'(u)\varphi := \begin{bmatrix} v\cdot\nabla w + \nabla q \\ 0 \end{bmatrix}.$$

With this notation, we introduce the stabilized form

$$A_\delta(u_h; \varphi_h) := A(u_h; \varphi_h) + (A(u_h) - F, S(u_h)\varphi_h)_\delta,$$

with $S(u_h) := \tilde{A}'(u_h)$ and the mesh-dependent inner product and norm

$$(v,w)_\delta := \sum\nolimits_{T\in\mathcal{T}_h} \delta_K\,(v,w)_K, \quad \|v\|_\delta = (v,v)_\delta^{1/2}.$$

The stabilization parameter is chosen according to

$$\delta_K = \alpha\big(\nu h_K^{-2}, \beta\,|v_h|_{K;\infty} h_K^{-1}\big)^{-1}, \quad \delta := \max_{K\in\mathcal{T}_h} \delta_K, \tag{4.28}$$

with the heuristic choice $\alpha = \frac{1}{12}$, $\beta = \frac{1}{6}$. Now, in the discrete problems, we seek $\{p_h, v_h\} \in V_h + \hat{v}_h$, such that

$$A_\delta(u_h;\varphi_h) = F(\varphi_h) \quad \forall \varphi_h \in V_h. \tag{4.29}$$

This approximation is fully consistent in the sense that the exact solution $u = \{p, v\}$ also satisfies (4.29). This implies again Galerkin orthogonality (2.3) for the error $e = \{e^p, e^v\} := \{p - p_h, v - v_h\}$ with respect to the form $A_\delta(\cdot;\cdot)$. We note that there are other possible choices of the stabilizing operator in the form $A_\delta(\cdot;\cdot)$, e.g., $S = -\tilde{A}'(u)^*$ (see the compressible flow example below).

Usually the adjustment of the mesh $\mathcal{T}_h = \{K\}$ is oriented by the size of certain local "error indicators" $\eta_K = \eta_K(v,p)$ which can cheaply be obtained from the computed solution $\{v_h, p_h\}$. Common candidates of *heuristic* indicators are

- *Vorticity*: $\eta_K := \|\nabla \times v_h\|_K$,
- *Pressure-gradient*: $\eta_K := \|\nabla p_h\|_K$,
- *"Energy-error"*: $\eta_K := \|R_h\|_K + h_K^{1/2}\|[\partial_n v_h]\|_{\partial K} + \|\nabla\cdot v_h\|_K$, with the "equation residual" $R_h := -\nu\Delta v_h + v_h\cdot\nabla v_h + \nabla p_h$.

The vorticity and the pressure-gradient indicators measure the "smoothness" of the computed solution $\{v_h, p_h\}$ while the "energy-error" indicator additionally contains information concerning local conservation of mass and momentum.

In Fig. 1.4, we compare the results for approximating the drag coefficient $J_{\text{drag}}(v,p)$ on meshes which are constructed by using the different error indicators with that obtained on uniformly refined meshes. It turns out that all the above indicators perform equally weakly. A better result is obtained by using a "weighted indicator", $\eta_K := \rho_K\cdot\omega_K$ in which the three residual terms contained in the "energy-error" indicator are multiplied by weights ω_K which are obtained from the solution of a global dual problem (generalized Green function) and represent the sensitivity of the error $J_{\text{drag}}(v,p) - J_{\text{drag}}(v_h,p_h)$ with respect to changes of the residuals ρ_K under mesh refinement. The basis of this approach is

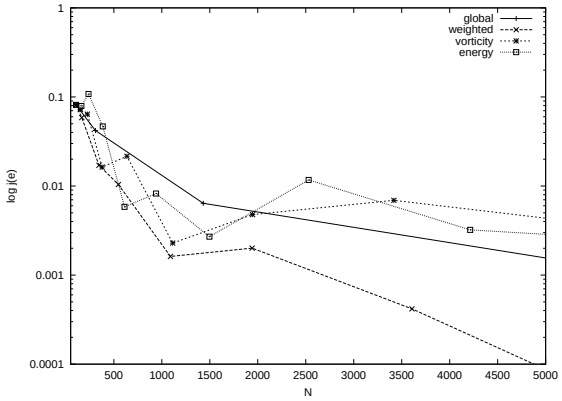

Fig. 1.4. Mesh efficiency obtained by global uniform refinement ("global" +), the weighted indicator ("weighted" $\times$), the vorticity indicator ("vorticity" $*$), and the energy indicator ("energy" $\Box$).

provided by the abstract Theorem 1.2.1 applied to the present concrete situation. Here, for simplicity, the explicit dependence of the stabilization parameter δ on the solution is neglected.

Theorem 1.4.1 *For a (linear) functional $J(\cdot)$ let $z = \{z^p, z^v\} \in V$ be the solution of the linearized dual problem*

$$A'_\delta(u_h; \varphi, z) = J(\varphi) \quad \forall \varphi \in V\,. \tag{4.30}$$

Then, there holds the a posteriori error estimate

$$|J(e)| \le \sum_{K \in \mathcal{T}_h} \Big\{ \sum_{i=1}^{3} \rho_K^{(i)} \omega_K^{(i)} + ... \Big\} + |R(u, u_h; e, e, z)|, \tag{4.31}$$

where

$$\begin{aligned}
\rho_K^{(1)} &= \|R^p(u_h)\|_K, & \omega_K^{(1)} &= \|z^p - z_h^p\|_K, \\
\rho_K^{(2)} &= \|R^v(u_h)\|_K, & \omega_K^{(3)} &= \|z^v - z_h^v\|_K + \delta_K \|\tilde{A}'(u_h)(z - z_h)\|_K\,, \\
\rho_K^{(3)} &= \|r^v(u_h)\|_{\partial K}, & \omega_K^{(3)} &= \|z^v - z_h^v\|_{\partial K},
\end{aligned}$$

with the cell and edge residuals

$$R^v(u_h)_{|K} := f + \nu \Delta v_h - v_h \cdot \nabla v_h - \nabla p_h\,, \quad R^p(u_h)_{|K} := \nabla \cdot v_h\,,$$

$$r^v(u_h)_{|\Gamma} := \begin{cases} -\frac{1}{2}[\nu \partial_n v_h - p_h n], & \text{if } \Gamma \not\subset \partial\Omega, \\ -(\nu \partial_n v_h - p_h n), & \text{if } \Gamma \subset \partial\Omega, \end{cases}$$

with $[\cdot]$ *denoting again the jump accross an interior edge* Γ, *and the nodal interpolant* $z_h = I_h z \in V_h$. *The dots "..." in (4.31) stand for additional terms measuring the errors in approximating the inflow data and the curved cylinder boundary which are neglected. The remainder term can be bounded by*

$$|R(u,u_h;e,e,z)| \;\le\; 2\,\|e^v\|\|\nabla e^v\|\|z^v\|_\infty + \mathcal{O}(\delta\|e^v\|)\,. \tag{4.32}$$

Proof. Neglecting the errors due to the approximation of the inflow boundary data $\hat{v}$ as well as the curved cylinder boundary S, we have to evaluate the residual $\langle\rho(u_h),\varphi\rangle := F(u_h,\varphi) - A_\delta(u_h,\varphi)$ for $\varphi = \{q,w\} \in V$. By definition, there holds

$$\begin{aligned}\langle\rho(u_h),\varphi\rangle \;&= (f,w) - \nu(\nabla v_h,\nabla w) - (v_h{\cdot}\nabla v_h, w) + (p_h,\nabla{\cdot}w)\\ &\quad - (q,\nabla{\cdot}u_h) - (A(u_h){-}F, \tilde{A}'(u_h)\varphi)_\delta.\end{aligned}$$

Splitting the integrals into their contributions from each cell $K \in \mathcal{T}_h$ and integrating cellwise by parts yields analogously as in deriving (3.18):

$$\begin{aligned}\langle\rho(u_h),\varphi\rangle \;&= \sum\nolimits_{K\in\mathcal{T}_h}\Big\{(R(u_h),w)_K + (r(u_h),w)_{\partial K} + (q,\nabla{\cdot}v_h)_K\\ &\quad + \delta_K(R(u_h), v_h{\cdot}\nabla w + \nabla q)_K\Big\}.\end{aligned}$$

From this, we obtain the error estimate (4.31) if we set $\varphi := z - I_h z$.

It remains to estimate the remainder term $R(u,u_h;e,e,z)$. The first derivative of $A_\delta(\cdot;\cdot)$ has for arguments $u=\{p,v\}$, $\varphi=\{q,w\} \in V$ and $z=\{z^p,z^v\} \in V$ the explicit form

$$A'_\delta(u;\varphi,z) \;=\; (A'(u)\varphi,z) + (A'(u)\varphi,\tilde{A}'(u)z)_\delta + (A(u),\tilde{A}''(u)\varphi z)_\delta,$$

with $A'(u)\varphi$ and $\tilde{A}'(u)z$ defined as above. Further, we note that

$$\tilde{A}''(u)\varphi z := \begin{bmatrix} w{\cdot}\nabla z^v \\ 0 \end{bmatrix}, \quad A''(u)\psi\varphi := \begin{bmatrix} \phi{\cdot}\nabla w + w{\cdot}\nabla\phi \\ 0 \end{bmatrix}.$$

Since $\tilde{A}'''(u) \equiv 0$, the second derivative of $A_\delta(\cdot;\cdot)$ has for arguments $u=\{p,v\}$, $\psi=\{\chi,\phi\}$, $\varphi=\{q,w\} \in V$ and $z=\{z^p,z^v\} \in V$ the form

$$\begin{aligned}A''_\delta(u;\psi,\varphi,z) \;&= (\phi{\cdot}\nabla w{+}w{\cdot}\nabla\phi, z^v) + (A''(u)\psi\varphi, \tilde{A}'(u)z)_\delta\\ &\quad + 2\,(A'(u)\varphi, \tilde{A}''(u)\psi z)_\delta\\ &= (\phi{\cdot}\nabla w{+}w{\cdot}\nabla\phi, z^v) + (\phi{\cdot}\nabla w{+}w{\cdot}\nabla\phi{+}\nabla q, v{\cdot}\nabla z^v)_\delta\\ &\quad + 2\,(-\nu\Delta w{+}v{\cdot}\nabla w{+}w{\cdot}\nabla v, \phi{\cdot}\nabla z^v)_\delta\,.\end{aligned}$$

From this, we easily infer the proposed bound for the remainder term by applying Hölder's inequality. □

In the estimate (4.31) the additional terms representing the errors in approximating the inflow data and the curved boundary component S are neglected; they can be expected to be small compared to the other residual terms. The bounds for the dual solution $\{z^p, z^v\}$ are obtained computationally by replacing the unknown velocity v in in the derivative form $A'(v;\cdot,\cdot)$ by its approximation v_h and solving the resulting linearized problem on the same mesh. From this approximate dual solution $\tilde{z}_h$, patchwise biquadratic interpolations are taken to approximate z in evaluating the weights $I_h^{(2)}\tilde{z}_h - z_h \approx z - z_h$. This frees us from choosing any interpolation constants.

The quantitative results of Fig. 1.4 and the corresponding meshes shown in Fig. 1.5 confirm the superiority of the weighted error indicator in computing local quantities.

We note that in our computation the drag coefficient has been evaluated from the formula

$$J_{\rm drag}(v,p) := \frac{2}{\hat{V}^2 D}\int_\Omega \left\{\sigma(p,v)\nabla\bar{\psi} + \nabla\cdot\sigma(p,v)\bar{\psi}\right\} dx\,, \tag{4.33}$$

where $\bar{\psi}$ is an extension of the directional vector $\psi := (0,1)^T$ from S to Ω with support along S. By integration by parts, one sees that this definition is independent of the choice of $\bar{\psi}$ and that it is equivalent to the original one (4.26) as a contour integral. However, on the discrete level the two formulations differ. In fact, computational experience shows that formula (4.33) yields significantly more accurate approximations of the drag coefficient (see [13] and [4]).

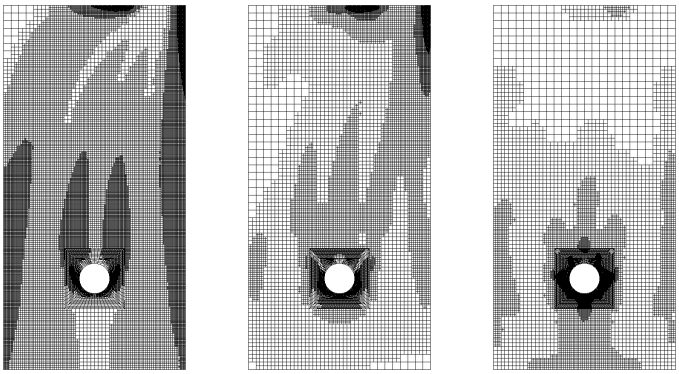

Fig. 1.5. Meshes with about 5,000 cells obtained by the vorticity indicator (left), the "energy" indicator (middle), and the weighted indicator (right).

1.5 Application to "low-Mach-number" compressible flow

As the second application, we consider low-Mach-number compressible gas flow with density variations due to temperature gradients. Such conditions often occur in chemically reactive flows and are characterized by hydrodynamically incompressible behavior . For the application of our approach to such problems see [10], [7], [6], and [11]. As a typical example (without chemistry), we choose a 2D benchmark "heat-driven cavity" (for details see Fig. 1.6 and [19] or [5]). Here, the flow, confined to a square box with side length $L = 1$, is driven by a temperature difference $T_h - T_c = 2\varepsilon T_0$ between the left ("hot") and the right ("cold") wall under the action of gravity g in the y-direction.

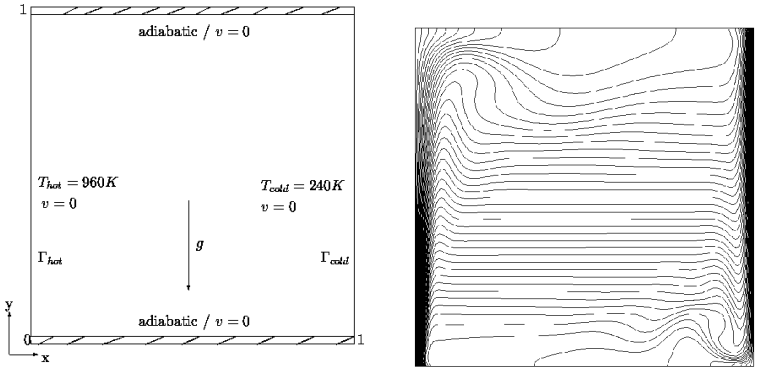

Fig. 1.6. Configuration of the heat-driven cavity problem and plot of computed temperatur isolines.

For the viscosity μ Sutherland's law is used,

$$\mu(T) \;=\; \mu^*\Big(\frac{T}{T^*}\Big)^{1/3}\frac{T^*+S}{T+S},$$

with the Prandtl number $\mathrm{Pr}=0.71$, $T^* = 273\,K$, $\mu^* = 1.68{\cdot}10^{-5}\mathrm{kg/ms}$, and $S := 110.5\,K$. Further, the heat conductivity is $\kappa(T) = \mu(T)/\mathrm{Pr}$. In the stationary case the thermodynamic pressure is defined by

$$P_{\mathrm{th}} \;=\; P_0\Big(\int_\Omega T_0^{-1}\,dx\Big)\Big(\int_\Omega T^{-1}\,dx\Big)^{-1},$$

where $T_0 = 600\,K$ is a reference temperature and $P_0 = 101,325\,\mathrm{Pa}$. Accordingly, the Rayleigh number is determined by

$$\mathrm{Ra} \;=\; \mathrm{Pr}\,g\Big(\frac{\rho_0 L}{\mu_0}\Big)^2\frac{T_h-T_c}{T_0} \;\approx\; 10^6, \qquad \varepsilon \;=\; \frac{T_h-T_c}{T_h+T_c} \;=\; 0.6\,,$$

where $\mu_0 := \mu(T_0)$, $\rho_0 := P_0/RT_0$, and $R = 287\,\mathrm{J/kgK}$. The boundary conditions are "no slip" for the velocity along the whole boundary, adiabatic (Neumann) boundary conditions for the temperature along the upper and lower wall and Dirichlet conditions for the temperature along the left and right hand walls which are represented by a function $\hat{T}$.

In this benchmark, one of the quantities to be computed is the average Nusselt number along the cold wall:

$$J(u) := c \int_{\Gamma_{\mathrm{cold}}} \kappa \partial_n T \, ds, \quad c := \frac{\mathrm{Pr}}{2\mu_0 T_0 \varepsilon}.$$

The mathematical model is the set of the (stationary) compressible Navier-Stokes equations in the so-called "low-Mach-number approximation" due to the low speed of the resulting flow. Accordingly, the total pressure is split like $P(x) = P_{\mathrm{th}} + p(x)$ into a thermodynamical part P_{th} which is constant in space and used in the gas law, and a hydrodynamic part $p(x) \ll P_{\mathrm{th}}$ used in the momentum equation. Then, the governing system of conservation equations can be written in the following form:

$$\begin{aligned} \nabla\cdot v - T^{-1} v\cdot\nabla T &= 0, \\ \rho v\cdot\nabla v + \nabla\cdot\tau + \nabla p &= (\rho-\rho_0)\, g, \\ \rho v\cdot\nabla T - \nabla\cdot(\kappa\nabla T) &= f_T, \end{aligned} \tag{5.34}$$

supplemented by the law of an ideal gas $\rho = P_{\mathrm{th}}/RT$. The stress tensor is given by $\tau = -\mu\{\nabla v + (\nabla v)^T - \frac{2}{3}(\nabla\cdot v) I\}$. In the present model case there are no heat sources (e.g., due to chemical reactions), i.e., $f_T = 0$. The variational formulation of (5.34) uses the following semi-linear form defined for triples $u = \{p, v, T\}$, $\varphi = \{q, w, \xi\}$:

$$\begin{aligned} A(u;\varphi) &:= (\nabla\cdot v - T^{-1} v\cdot\nabla T, q) + (\rho v\cdot\nabla v, w) - (\tau, \nabla w) - (p, \nabla\cdot w) \\ &\quad - (p, \nabla\cdot w) - (\rho g, w) + (\rho v\cdot\nabla T, \xi) + (\kappa\nabla T, \nabla\xi). \end{aligned}$$

Further, we define the functional

$$F(\varphi) := -(\rho_0 g, w).$$

The natural solution spaces are $\hat{V} := L^2(\Omega)/\mathbb{R} \times H^1(\Omega)^2 \times H^1(\Omega)$ and $V := L^2(\Omega)/\mathbb{R} \times H_0^1(\Omega)^2 \times H_0^1(\Gamma_y;\Omega)$, where $H_0^1(\Gamma_y;\Omega) := \{\xi \in H^1(\Omega),\, \xi_{|x\in\{0,L\}} = 0\}$. With this notation, the variational form of (5.34) seeks $u = \{p, v, T\} \in V + \hat{u}$, with $\hat{u} = \{0, 0, \hat{T}\}$, satisfying

$$A(u;\varphi) = F(\varphi) \quad \forall \varphi \in V, \tag{5.35}$$

where the density ρ is considered as a (nonlinear) coefficient determined by the temperature through the equation of state $\rho = P_{\mathrm{th}}/RT$.

The discretization of the system (5.35) uses again the continuous Q_1-finite element for all unknowns and employs least-squares stabilization for the velocity-pressure coupling as well as for the transport terms. We do not state the corresponding discrete equations since they have an analogous structure as already seen in the preceding section for the incompressible Navier-Stokes equations. The derivation of the related (linearized) dual problem and the resulting a posteriori error estimates follows the same line of argument. For economy reasons, we do not use the full Jacobian of the coupled system in setting up the dual problem, but only include its dominant parts. The same simplification is used in the nonlinear iteration process. For details, we refer to [7], [11], and particularly the recent paper [5].

The discrete problems seek $u_h = \{p_h, v_h, T_h\} \in V_h + \hat{u}_h$, satisfying

$$A_\delta(u_h; \varphi_h) = F(\varphi_h) \quad \forall \varphi_h \in V_h, \tag{5.36}$$

with the stabilized form

$$A_\delta(u_h; \varphi_h) := A(u_h; \varphi_h) + (A(u_h), S(u_h)\varphi_h)\,.$$

As on the continuous level the discrete density is determined by the temperature through the equation of state $\rho_h := P_{\rm th}/RT_h$. Here, the operator $A(u_h)$ is the generator of the form $A(u_h; \cdot)$, and the operator $S(u_h)$ in the stabilization term is chosen according to $S(u_h) := -\tilde{A}'(u_h)^*$ where $\tilde{A}'(u_h)$ represents the differential part of $A'(u_h) = \tilde{A}'(u_h) + A_0'(u_h)$, while $A_0'(u_h)$ contains all zero-order terms. Accordingly, we have

$$S(u_h) := \begin{bmatrix} 0 & \mathrm{div} & 0 \\ \nabla & \rho_h v_h\cdot\nabla + \nabla\cdot\mu\nabla & 0 \\ -T_h^{-1} v_h\cdot\nabla & 0 & \rho_h v_h\cdot\nabla + \nabla\cdot\kappa\nabla \end{bmatrix}.$$

We introduce the following notation for the equation residuals of the solution $u_h = \{p_h, v_h, T_h\}$ of (5.36):

$$\begin{aligned} R^p(u_h) &= \nabla\cdot v_h - T_h^{-1} v_h\cdot\nabla T_h\,, \\ R^v(u_h) &= \rho_h v_h\cdot\nabla v_h - \nabla\cdot(\mu\nabla v_h) + \nabla p_h + (\rho_0 - \rho_h)g\,, \\ R^T(u_h) &= \rho_h v_h\cdot\nabla T_h - \nabla\cdot(\kappa\nabla T_h) - f_T\,. \end{aligned}$$

Then, the stabilizing part in $A_\delta(\cdot;\cdot)$ can be written in the form

$$\begin{aligned} (A(u_h), S(u_h)\varphi_h)_\delta &= (R^p(u_h), \nabla\cdot w)_\delta \\ &\quad + (R^v(u_h), \nabla q + \rho_h v_h\cdot\nabla w + \nabla\cdot(\mu\nabla w))_\delta \\ &\quad + (R^T(u_h), \rho_h v_h\cdot\nabla\xi + \nabla\cdot(\kappa\nabla\xi) - T_h^{-1} v_h\cdot\nabla q)_\delta\,, \end{aligned}$$

for $\varphi = \{q, w, \xi\}$. These terms comprise stabilization of the stiff pressure-velocity coupling in the low-Mach-number situation as well as stabilization of transport in the momentum and energy equation. The parameters $\delta_K = \{\delta_K^p, \delta_K^v, \delta_K^T\}$ may be chosen differently in the three equations following rules analogous to (4.28). The stability of this discretization has been investigated in [5].

From Theorem 1.2.1, we obtain the following result by the same argument as used in Theorem 1.4.1. This analysis assumes for simplicity that viscosity μ and heat conductivity κ are determined by T_0.

Theorem 1.5.1 *For a (linear) functional $J(\cdot)$ let $z = \{z^p, z^v, z^T\} \in V$ be the solution of the linearized dual problem*

$$A'_\delta(u_h; \varphi, z) = J(\varphi) \quad \forall \varphi \in V\,. \tag{5.37}$$

Then, there holds the a posteriori error estimate

$$|J(e)| \le \sum_{K\in\mathcal{T}_h} \Big\{ \sum_{i=1}^{5} \rho_K^{(i)} \omega_K^{(i)} \Big\} + |R(u, u_h; e, e, z)|, \tag{5.38}$$

where

$$\begin{aligned}
\rho_K^{(1)} &= \|R^p(u_h)\|_K, & \omega_K^{(1)} &= \|z^p - z_h^p\|_K + \delta_K^p \|S^p(u_h)(z^p - z_h^p)\|_K,\\
\rho_K^{(2)} &= \|R^v(u_h)\|_K, & \omega_K^{(2)} &= \|z^v - z_h^v\|_K + \delta_K^v \|S^v(u_h)(z^v - z_h^v)\|_K\,,\\
\rho_K^{(3)} &= \|r^v(u_h)\|_{\partial K}, & \omega_K^{(3)} &= \|z^v - z_h^v\|_{\partial K},\\
\rho_K^{(4)} &= \|R^T(u_h)\|_K, & \omega_K^{(4)} &= \|z^T - z_h^T\|_K + \delta_K^T \|S^T(u_h)(z^T - z_h^T)\|_K\,,\\
\rho_K^{(5)} &= \|r^T(u_h)\|_{\partial K}, & \omega_K^{(5)} &= \|z^T - z_h^T\|_{\partial K},
\end{aligned}$$

with the cell and edge residuals

$$\begin{aligned}
R^p(u_h)_{|K} &:= \nabla\cdot v_h - T_h^{-1} v_h\cdot\nabla T_h\,,\\
R^v(u_h)_{|K} &:= \rho_h v_h\cdot\nabla v_h - \nabla\cdot(\mu\nabla v_h) + \nabla p_h + (\rho_0 - \rho_h) g\,,\\
r^v(u_h)_{|\Gamma} &:= \begin{cases} -\frac{1}{2}[\nu\partial_n v_h - p_h n], & \text{if } \Gamma \not\subset \partial\Omega,\\ -(\nu\partial_n v_h - p_h n), & \text{if } \Gamma \subset \partial\Omega, \end{cases}\\
R^T(u_h)_{|K} &:= \rho_h\cdot\nabla T_h - \nabla\cdot(\kappa\nabla T_h)\,,\\
r^T(u_h)_{|\Gamma} &:= \begin{cases} -\frac{1}{2}[\kappa\partial_n T_h], & \text{if } \Gamma \not\subset \partial\Omega,\\ -\kappa\partial_n T_h, & \text{if } \Gamma \subset \partial\Omega, \end{cases}
\end{aligned}$$

with $[\cdot]$ denoting again the jump accross an interior edge Γ, and the nodal interpolant $z_h = I_h z \in V_h$. The remainder term can be bounded analogously as in Theorem 1.4.1 for incompressible flow.

In Fig. 1.7 and Table 1.1, we demonstrate the mesh efficiency of the "weighted" error indicator compared to a heuristic "energy-error" indicator similar to the one discussed in Section 1.4 for the incompressible flow case. A collection of refined meshes produced by the two error indicators is shown in Fig. 1.8. The superiority of the "weighted" indicator is particularly evident if higher solution accuracy is required. As usual in problems of such complex structure, the a posteriori bound $\eta(u_h)$ tends to over-estimate the true error but it appears to be "reliable" and the "effectivity index" $I_{\text{eff}} := \eta/e$ stays of the order $\mathcal{O}(1)$ as $N \to \infty$.

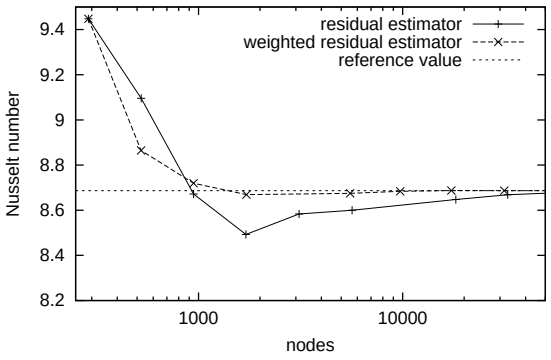

Fig. 1.7. Results of computing the Nusselt number by using the "residual indicator" (symbol "+") and the "weighted residual indicator" (symbol "×").

Table 1.1. *Results for the computation of the Nusselt number by the "energy-error" indicator (left) and the weighted error indicator (right).*

N	$\langle Nu \rangle_c$	e
289	-9.44783	7.6e-01
524	-9.09552	4.1e-01
945	-8.67201	1.5e-02
1708	-8.49286	1.9e-01
3108	-8.58359	1.0e-01
5656	-8.59982	8.7e-02
18204	-8.64775	3.9e-02
32676	-8.66867	1.8e-02
58678	-8.67791	8.7e-03
79292	-8.67922	7.4e-03

N	$\langle Nu \rangle_c$	e	η
289	-9.44783	7.6e-01	7.9e-01
523	-8.86487	1.8e-01	3.4e-01
945	-8.71941	3.3e-02	1.5e-01
1717	-8.66898	1.8e-02	6.6e-02
5530	-8.67477	1.2e-02	2.1e-02
9728	-8.68364	3.0e-03	1.1e-02
17319	-8.68744	8.5e-04	6.3e-03
31466	-8.68653	6.9e-05	3.7e-03
56077	-8.68653	6.7e-05	2.1e-03
78854	-8.68675	1.5e-04	1.5e-03

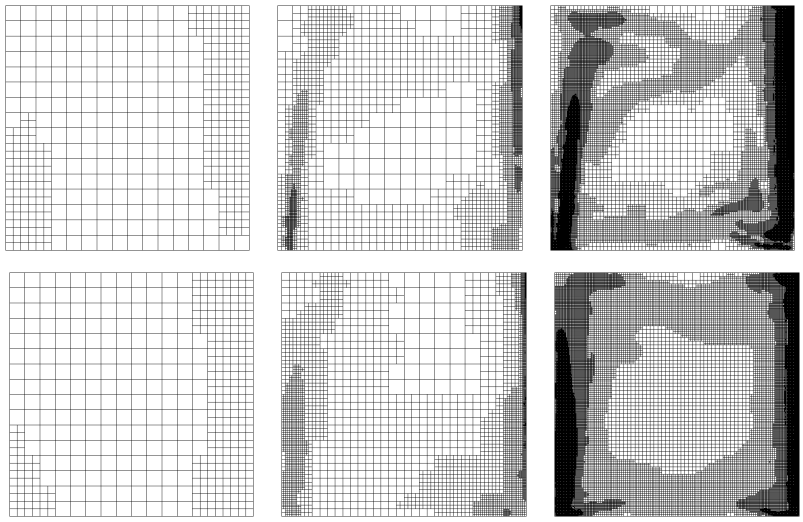

Fig. 1.8. Sequences of refined meshes obtained by the "energy-error" indicator (upper row, $N = 524, 5656, 58678$) and the weighted error estimator (lower row, $N = 523, 5530, 56077$).

References

[1] Ainsworth, M. and Oden, J.T. (1997). A posteriori error estimation in finite element analysis. *Comput. Methods Appl. Mech. Engrg.*, 142:1–88.

[2] Becker, R. (1995). *An Adaptive Finite Element Method for the Incompressible Navier-Stokes Equations on Time-Dependent Domains.* Thesis, Preprint 95-44, SFB 359, Univ. Heidelberg.

[3] Becker, R. (1998). An adaptive finite element method for the Stokes equations including control of the iteration error. *Proc. ENUMATH-97* (H. G. Bock, et al., eds.), pp. 609–620, World Scient. Publ., Singapore, 1998.

[4] Becker, R. (1998). Weighted error estimators for the incompressible Navier-Stokes equations Technical Report 98-20, SFB 359, Univ. Heidelberg.

[5] Becker, R. and Braack, M. (2000). Fast computation of compressible flows at low Mach number with finite elements. Technical Report, SFB 359, Univ. Heidelberg, June, 2000.

[6] Becker, R., Braack, M., Rannacher, R. and Waguet, C. (1999). Fast and reliable solution of the Navier-Stokes equations including chemistry. *Computing and Visualization in Science*, 2:107–122.

[7] Becker, R., Braack, M. and Rannacher, R. (1999). Numerical simulation of laminar flames at low Mach number with adaptive finite elements. *Combustion Theory and Modelling*, 3:503–534.

[8] Becker, R. and Rannacher, R. (1998). Weighted a posteriori error control in FE methods. ENUMATH-95, Paris, 1995, *Proc. ENUMATH-97*, H. G. Bock, et al., eds., pp. 621–637, World Scient. Publ., Singapore.

[9] Becker, R. and Rannacher, R. (1996). A feed-back approach to error control in finite element methods: basic analysis and examples. *East-West J. Numer. Math.*, 4:237-264.

[10] Braack, M. (1998). *An Adaptive Finite Element Method for Reactive Flow Problems*. Dissertation, Univ. Heidelberg, 1998.

[11] Braack, M. and Rannacher, R. (1999), Adaptive finite element methods for low-Mach-number flows with chemical reactions, Lecture Series 1999-03, *30th Computational Fluid Dynamics*, (H. Deconinck, ed.), von Karman Institute for Fluid Dynamics, Belgium.

[12] Eriksson, K., Estep, D., Hanspo, P. and Johnson, C. (1995). Introduction to adaptive methods for differential equations. *Acta Numerica 1995* (A. Iserles, ed.), pp. 105-158, Cambridge University Press.

[13] Giles, M., Larsson, M., Levenstam, M. and Süli, E. (1997). Adaptive error control for finite element approximations of the lift and drag coefficients in viscous flow. Technical Report, NA-76/06, Oxford University Computing Laboratory *SIAM J. Numer. Anal.*, to appear.

[14] Houston, P., Rannacher, R. and Süli, E. (1999). A posteriori error analysis for stabilised finite element approximation of transport problems. *Compu. Meth. Appl. Sci. Engrg.*, to appear.

[15] Hughes, T. J. R. and Brooks, A. N. (1982). Streamline upwind/Petrov Galerkin formulations for convection dominated flows with particular emphasis on the incompressible Navier-Stokes equation. *Comp. Math. Appl. Mech. Eng.*, 32:199–259.

[16] Hughes, T. J. R., Franca, L. P. and Balestra, M. (1986). A new finite element formulation for computational fluid dynamics: V. Circumvent the Babuska-Brezzi condition: A stable Petrov-Galerkin formulation for the Stokes problem accomodating equal order interpolation. *Comp. Meth. Appl. Mech. Eng.*, 59:89–99.

[17] Johnson, C. (1987). *Numerical Solution of Partial Differential Equations by the Finite Element Method*, Cambridge University Press, Cambridge-Lund.

[18] Johnson, C. (1993). A new paradigm for adaptive finite element methods. *Proc. MAFELAP Conf.*, Brunel Univ. 1993, John Wiley.

[19] Le Quere, P. and Paillere,H. (2000). Modelling an simulation of natural convection flows with large temperature differences: a benchmark problem for low Mach number solvers, *Int. J. Thermal Sciences*, to appear.

[20] Rannacher, R. (1999). Error control in finite element computations. Proc. Summer School on *Error Control and Adaptivity in Scientific Computing* (H. Bulgak and C. Zenger, eds.), pp. 247–278, Kluwer Academic Publishers.

[21] Schäfer, M. and Turek, S. (1996). The benchmark problem "flow around a cylinder". *Flow Simulation with High-Performance Computers*, E.H. Hirschel, ed., Notes Comput. Fluid Mech., Vieweg, Stuttgart.

[22] Verfürth, R. (1996). *A Review of A Posteriori Error Estimation and Adaptive Mesh-Refinement Techniques*, Wiley/Teubner, New York–Stuttgart.